Research in Astronomy and Astrophysics, 23:095015 (9pp), 2023 September https://doi.org/10.1088/1674-4527/acd52f

Variable Star Detection in the Field of Open Cluster NGC 188

Fang-Fang Song[1,2], Hu-Biao Niu[1,2], Ali Esamdin[1,2], Yu Zhang[1,2], and Xiang-Yun Zeng[3]
[1] Xinjiang Astronomical Observatory, Chinese Academy of Sciences, Urumqi 830011, China; niuhubiao@xao.ac.cn
[2] School of Astronomy and Space Science, University of Chinese Academy of Sciences, Beijing 100049, China
[3] Center for Astronomy and Space Sciences, China Three Gorges University, Yichang 443000, China
Received 2023 March 14; revised 2023 April 13; accepted 2023 April 23; published 2023 August 8

Abstract

This work presents the charge-coupled device (CCD) photometric survey of the old open cluster NGC 188. Time-series *V*-band photometric observations were conducted for ten nights in 2017 January using the Nanshan One-meter Wide-field Telescope to search for variable stars in the field of the cluster. A total of 25 variable stars, including one new variable star, were detected in the target field. Among the detected variables, 16 are cluster member stars, and the others are identified as field stars. The periods, radial velocities, effective temperatures, and classifications of the detected variables are discussed in this work. Most of the stars' effective temperatures are between 4200 and 6600 K, indicating their spectral types are G or K. The newly discovered variable is probably a W UMa system. In this study, a known cluster variable star (V21=V0769 Cep) is classified as an EA-type variable star based on the presence of an 0.5 mag eclipse in its light curve.

Key words: (stars:) binaries: general – stars: general – (Galaxy:) open clusters and associations: individual (NGC 188) – stars: variables: general

1. Introduction

Open clusters (OCs), which are composed of young stars, are crucial for studying the formation and evolution of the stellar populations and Galactic disk (Piskunov et al. 2006; Özeren et al. 2014; Gillen et al. 2020). Because the cluster members born from the same interstellar cloud are assumed to have a common age, distance, reddening and chemical abundance, the studies of cluster variables provide significant clues to probe the structure and evolution of stars and clusters. The high precision in the astrometric and photometric measurements by Gaia gives more opportunities to classify cluster member stars from field stars, which represents great progress for the studies of variable stars in OCs (Gaia Collaboration et al. 2016; Cantat-Gaudin et al. 2020).

As one of the most ancient, rich OCs known in our Milky Way, NGC 188 ($l = 122\overset{\circ}{.}843$, $b = +22\overset{\circ}{.}384$, C 0039+850) is a captivating OC that has been intensively investigated by numerous studies (Sarajedini et al. 1999; Friel et al. 2010; Hills et al. 2015; Cohen et al. 2020). It is an excellent laboratory based on its abundant member stars, being easy to observe and less contaminated by field stars owning to its special location that it is positioned at high latitude far away from the Galactic disk (Bonatto et al. 2005; Fornal et al. 2007; Wang et al. 2015); 857 cluster member stars with probabilities over 70% were identified by Cantat-Gaudin et al. (2020). Lists summarizing the previous observational surveys for the cluster are published in Fornal et al. (2007), Geller et al. (2008), Wang et al. (2015). Various works about the fundamental parameters of NGC 188 have been performed after the release of the Gaia data which provide unprecedentedly precise parallax measurements (Gaia Collaboration et al. 2018; Bonatto 2019; Cantat-Gaudin et al. 2020; Monteiro et al. 2020). Taking the fitted parameters by Cantat-Gaudin et al. (2020), the basic cluster parameters of NGC 188 are as follows: the distance modulus is 11.15 mag, corresponding to a distance of 1698 pc, log(Age) = 9.85 yr and extinction $A_V = 0.21$ mag.

Also, NGC 188 is a special cluster owning to its abundance and variety of variable stars. Early in the 1960s, four short-period W UMa stars (known as EQ Cep, ER Cep, ES Cep and EP Cep) and a suspected variable NSV 395 were discovered by Hoffmeister (1964). Kaluzny & Shara (1987) and Kaluzny (1990) found another seven short-period variables through charge-coupled device (CCD) photometric surveys using the 0.9 m telescope at Kitt Peak National Observatory (KPNO). Subsequently, Xin et al. (2002) and Zhang et al. (2004) published findings on sixteen variables by monitoring the cluster in a 1 deg^2 field with the 60/90 cm Schmidt telescope located at the Xinglong Station of the National Astronomical Observatories, Chinese Academy of Sciences (CAS). Meanwhile, Kafka & Honeycutt (2003) reported 51 faint variables in the cluster's central area of 17 × 17 arcmin^2 with WIYN 3.5m Telescope, but only two variables were detected by the subsequent monitoring of other telescopes. Another 18 variables were discovered by Mochejska et al. (2008) as the result of searching for transiting planets in the OC NGC 188, part of the project Planets in Stellar Clusters Extensive Search (PISCES). In the field of $1.5 \times 1.5\,\mathrm{deg}^2$ around the cluster,

Table 1
Journal of CCD Photometric Observations for NGC 188 Where N Represents the Number of Images and Exp Represents Observation Exposure Time for each Filter

UT date	Object	Pixel	Duration (Hr)	V ($N \times$ Exp)
05 Jan 2017	NGC 188	2900×2400	1.2	38×35 s
06 Jan 2017	NGC 188	2900×2400	1.8	58×35 s
07 Jan 2017	NGC 188	4096×4136	5.1	171×35 s
		2900×2400	2.6	110×35 s
08 Jan 2017	NGC 188	2600×2400	4.5	267×35 s
		2900×2400	5.4	290×35 s
09 Jan 2017	NGC 188	2900×2400	12.5	649×35 s
10 Jan 2017	NGC 188	2900×2400	12.5	657×35 s
11 Jan 2017	NGC 188	2900×2400	11.0	598×35 s
12 Jan 2017	NGC 188	2900×2400	0.7	67×35 s
13 Jan 2017	NGC 188	2900×2400	9.7	502×35 s
14 Jan 2017	NGC 188	2900×2400	12.5	666×35 s

18 new variable stars were identified by the MASTER series of robotic telescopes administered by the Astronomical Observatory of Ural Federal University (Popov et al. 2013). These variable stars were included in the electronic catalog of the American Association of Variable Star Observers (AAVSO/VSX[4]) in which 68 variable stars are known within a 30′ radius around NGC 188. The Gaia collaboration identified another 61 variable stars based on the Gaia Data Release 3 (DR3) database (Gaia Collaboration 2022). A total of 129 variables were collected in this field.

This paper is structured as follows. In Section 2 the observations and data reductions are presented. We focus on the variable identification and memberships in Section 3. In Section 4 we compare our results with previous works and emphasize our work on the new variable star. The conclusions are given in Section 5.

2. Observations and Data Reductions

In 2017 January, ten days of photometric observations were conducted by using the Nanshan One-meter Wide-field Telescope (NOWT; Song et al. 2016; Ma et al. 2018; Bai et al. 2020) located at the Nanshan station of Xinjiang Astronomical Observatory (XAO), CAS. An E2V CCD203-82 (blue) chip CCD camera with 4096×4136 pixels was mounted at the prime focus of the telescope, providing a field of view (FOV) of 1.3×1.3 deg^2. The telescope was equipped with a Johnson–Cousins standard *UBVIR* filter system for broadband photometry and operated at -120°C with liquid nitrogen cooling. During the observations, a number of bias and twilight flat frames were taken, and the seeing in all of these images was below 2.″2. In total, over 79 hr with 4198 images of useful data were obtained on 10 nights. The journal of the observations of NGC 188 is listed in Table 1. The exposure time of time-series observations for the V band is 35 s, and the typical FOV in this period is 54.62×45.2 arcmin^2, corresponding to 2900×2400 pixels. The observed field of NGC 188 is shown in Figure 1.

The data reduction steps followed the standard procedures employed for optical CCD aperture photometry. The observed images were pre-processed by IRAF[5] for overscan and bias subtraction and division for flat-field correction. The dark correction was ignored because the telescope was operated in a low-temperature environment and the thermionic noise was less than 1 e pix^{-1} h^{-1}. The instrumental magnitudes of the stars in each frame were extracted by the automated photometric software SExtractor (Bertin & Arnouts 1996) and the equatorial coordinates (R.A., decl.) for each detected star were computed by triangular matching with the UCAC4 catalog (Zacharias et al. 2013). Figure 2(a) represents the photometric errors of this work as a function of instrumental magnitudes in the V band, which indicate that the photometric errors are less than 0.1 mag when the observational magnitudes are brighter than 17 mag. Following the same procedure as described in Song et al. (2016); Ma et al. (2018); Li et al. (2021), the differential light curves of 3585 stars were obtained using the data processing system of our XAO time-domain survey pipeline.

3. Variable Identification

We examined the light curves of all detected stars by visual inspection and found 25 stars with obvious light variability. These variables were carefully examined for any blending or contamination by neighboring stars. The main characteristics of the 25 variable stars are listed in Table 2. The finding chart of these variable stars in the field of the cluster is displayed in Figure 1. These stars are not at the edge of CCD frames, and their light curves do not have outliers. The light variations of these variables can be seen in Figures 3 and 4. To investigate the spread in data points for variable stars, Figure 2(b) demonstrates the root-mean-square (rms, labeled as σ) scatter as a function of instrumental V magnitude. It indicates that, in general, detected variable stars (the red dots) have a larger standard deviation in magnitude compared to non-variable stars.

The periods of periodic variable stars were obtained by the generalized Lomb–Scargle (GLS) periodogram (Zechmeister & Kürster 2009) considering the effect of noise as a sub-package of PyAstronomy (Czesla et al. 2019). The GLS periodogram computes the error-weighted Lomb–Scargle periodogram, and provides more accurate frequencies compared with the Lomb–Scargle periodogram. The adopted periods correspond to the frequency of the maximum power and the accuracies of those

[4] http://www.aavso.org/vsx/

[5] Image Reduction and Analysis Facility, http://iraf.noao.edu/.

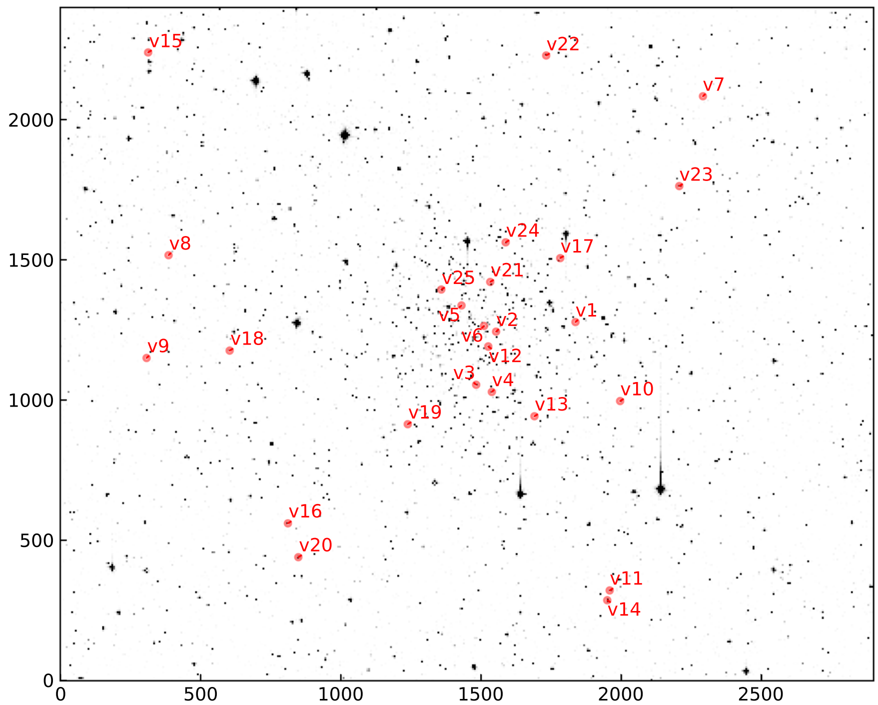

Figure 1. The field of NGC 188 observed using NOWT with the detected variable stars marked in red circles. North is up and east is to the left.

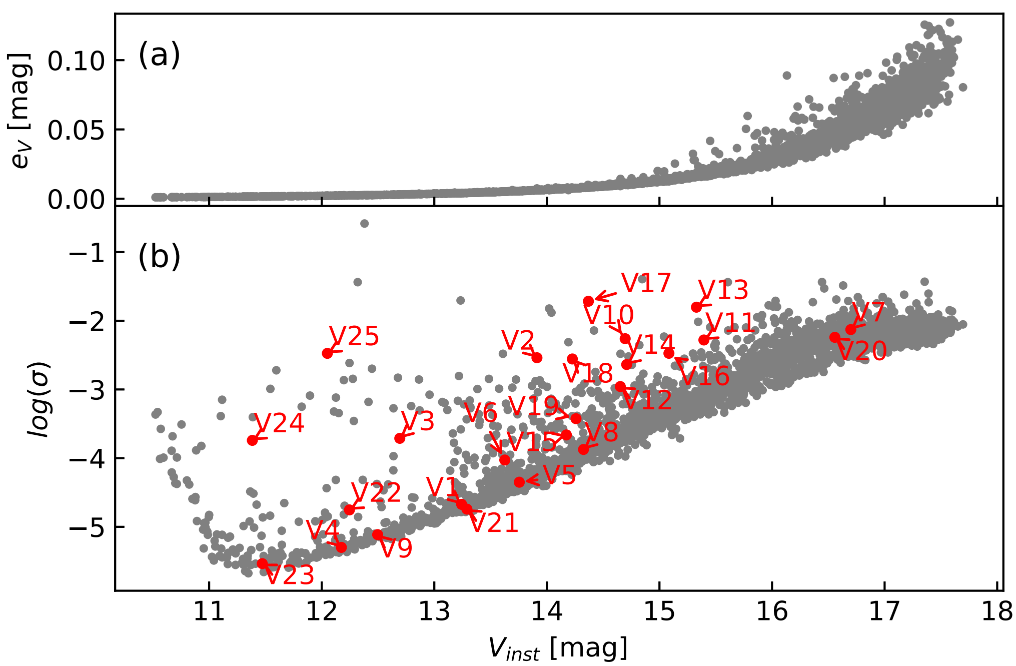

Figure 2. Panel (a) presents the photometric errors of this work as a function of instrumental magnitude in the *V* band, while panel (b) is the standard deviation as a function of magnitude. The red dots represent the variables stars identified in this work.

values are influenced by the mean magnitude, amplitude and measurement errors. To avoid false variability arising solely due to the aliasing effect, we rechecked all the calculated periods and none of them can be seen as a factor of one day. After binning in intervals of 0.01 phase, we calculate the mean magnitude in each bin. The resulting phase-folded light curves of periodic variables are plotted in Figures 3. Our data are insufficient to yield accurate periods for the other seven long-

Table 2
Basic Parameters of the Detected Variable Stars in the Field of the Open Cluster NGC 188

ID	Coords (J2000) (hh mm ss dd mm ss)	G (mag)	BP-RP (mag)	Distance (pc)	Parallax mas	pm RA mas yr^{-1}	pm DE mas yr^{-1}	Amplitude (mag)	Period (day)	Memb (yes/no?)	$T_{\rm eff}$ (K)	Type
V1	00 46 54.53 + 85 21 44.1	16.525(6)	1.12(2)	1587^{+98}_{-87}	0.58(4)	−2.47(5)	−0.84(4)	0.43(5)	0.28961(2)	yes	5423 ± 300	EW/KW
V2	00 47 33.92 + 85 16 24.8	16.49(1)	1.16(6)	1568^{+97}_{-86}	0.61(4)	−2.47(5)	−0.76(4)	0.83(6)	0.30675(2)	yes	5293 ± 261	EW/KW
V3	00 50 27.76 + 85 15 09.1	15.66(1)	1.05(5)	1214^{+43}_{-34}	0.80(3)	−0.09(4)	−1.88(3)	0.72(5)	0.28575(2)	no	5391 ± 155	EW/KW
V4	00 50 50.37 + 85 16 12.9	15.688(9)	1.06(4)	2077^{+87}_{-109}	0.47(3)	−2.44(3)	−0.79(3)	0.46(4)	0.34209(2)	yes	5502 ± 340	EW/KW
V5	00 46 12.12 + 85 14 02.0	16.14(1)	1.10(5)	1713^{+101}_{-86}	0.54(3)	−1.87(4)	−0.94(4)	0.44(9)	0.32849(4)	yes	5464 ± 270	EW/KW
V6	00 47 16.44 + 85 15 35.4	15.933(3)	1.04(1)	1758^{+78}_{-88}	0.54(3)	−2.24(4)	−0.98(3)	0.14(4)	0.33014(6)	yes	5447 ± 231	EW/KW
V7	00 33 48.89 + 85 29 22.3	15.147(7)	1.01(3)	1105^{+22}_{-25}	0.88(2)	6.05(2)	4.07(3)	0.45(4)	0.31602(2)	no	5552 ± 223	EW
V8	00 44 10.18 + 84 54 13.0	17.480(8)	1.84(5)	948^{+49}_{-46}	0.96(7)	−4.04(8)	−1.57(8)	0.8(1)	0.27707(4)	no	4252 ± 315	EW
V9	00 49 22.30 + 84 52 57.6	16.392(7)	1.01(2)	2990^{+344}_{-286}	0.31(4)	−1.38(5)	−0.61(4)	0.43(5)	0.38597(5)	yes	5578 ± 166	EW
V10	00 51 15.03 + 85 24 51.1	15.512(3)	0.97(1)	1716^{+92}_{-68}	0.55(2)	−2.24(3)	−0.60(3)	0.14(3)	0.35794(5)	yes	5648 ± 119	EW
V11	01 01 50.68 + 85 24 00.3	13.005(4)	0.793(8)	1029^{+271}_{-202}	0.6(3)	−9.4(3)	8.4(3)	0.11(4)	0.321(3)	no	⋯	EW
V12	00 48 22.88 + 85 15 54.9	15.826(5)	1.21(2)	2054^{+98}_{-72}	0.49(3)	−2.46(4)	−1.06(3)	0.31(4)	0.58426(8)	yes	5287 ± 458	EB
V13	00 52 08.76 + 85 19 05.9	17.622(4)	1.34(2)	1669^{+183}_{-128}	0.52(7)	−2.3(1)	−0.86(8)	0.2(1)	0.3048(3)	yes	4842 ± 358	EB
V14	01 02 23.28 + 85 23 49.1	13.49(1)	0.64(5)	3705^{+143}_{-131}	0.24(1)	8.21(1)	−0.95(1)	0.47(4)	0.4980(2)	no	6673 ± 228	RRAB
V15	00 34 05.31 + 84 51 59.0	14.106(6)	0.72(1)	1416^{+452}_{-261}	−1.2(6)	3.9(7)	2.4(8)	0.14(4)	0.23646(9)	no	⋯	RRC
V16	00 57 47.95 + 85 02 29.0	13.540(2)	0.889(6)	773^{+7}_{-6}	1.27(1)	−13.17(1)	7.97(2)	0.16(4)	0.873(2)	no	5673 ± 129	VAR
V17	00 43 23.96 + 85 20 32.5	14.986(3)	0.762(7)	1863^{+49}_{-48}	0.51(2)	−2.36(2)	−1.03(2)	0.05(3)	0.227(1)	yes	6246 ± 246	VAR
V18	00 48 54.43 + 84 58 31.6	15.492(3)	0.803(8)	1850^{+93}_{-76}	0.51(2)	5.33(3)	3.93(3)	0.09(4)	0.31698(9)	no	6116 ± 179	EW
V19	00 52 37.72 + 85 10 34.6	14.599(3)	0.888(6)	1841^{+84}_{-49}	0.51(2)	−2.27(2)	−0.82(2)	0.62(6)	⋯	yes	5888 ± 284	EA
V20	00 59 34.13 + 85 03 08.4	12.802(3)	0.835(5)	635^{+6}_{-5}	1.55(1)	8.11(2)	−5.79(2)	0.48(5)	⋯	no	5859 ± 105	EA
V21	00 44 52.20 + 85 15 54.3	15.596(3)	0.969(8)	1831^{+96}_{-102}	0.52(3)	−2.24(3)	−1.21(3)	0.51(6)	⋯	yes	5644 ± 128	EA
V22	00 32 21.20 + 85 18 38.0	14.341(4)	1.36(2)	1825^{+50}_{-43}	0.52(1)	−2.24(2)	−1.17(2)	0.13(3)	⋯	yes	4703 ± 143	L:
V23	00 39 00.88 + 85 28 15.4	13.319(4)	1.33(1)	3211^{+108}_{-125}	0.28(1)	−3.20(1)	1.29(1)	0.10(3)	⋯	no	4822 ± 231	L:
V24	00 42 40.49 + 85 16 49.4	15.005(3)	1.196(9)	1821^{+77}_{-65}	0.52(2)	−2.41(2)	−1.03(2)	0.10(3)	⋯	yes	5163 ± 316	LB
V25	00 45 23.00 + 85 12 38.0	13.770(4)	1.17(2)	1906^{+42}_{-47}	0.50(1)	−2.30(1)	−0.98(1)	0.23(3)	⋯	yes	5169 ± 296	RS:

Note. The classification of variable stars follows the same abbreviations of variable star types as listed in the VSX catalog. EW/KW indicate contact systems of W Ursae Majoris-type eclipsing variables; EB means β Lyrae-type eclipsing systems; EA signifies β Persei-type (Algol) eclipsing systems; RS corresponds to RS Canum Venaticorum-type binary systems; VAR denotes a variable star of unspecified type; RRAB indicates RR Lyrae variables with asymmetric light curves, while RRC means RR Lyrae variables with nearly symmetric light curves; L signifies slow irregular variables, while LB corresponds to slow irregular variables of late spectral types. In addition, colons after some types indicate that the type of the variable star is not yet determined.

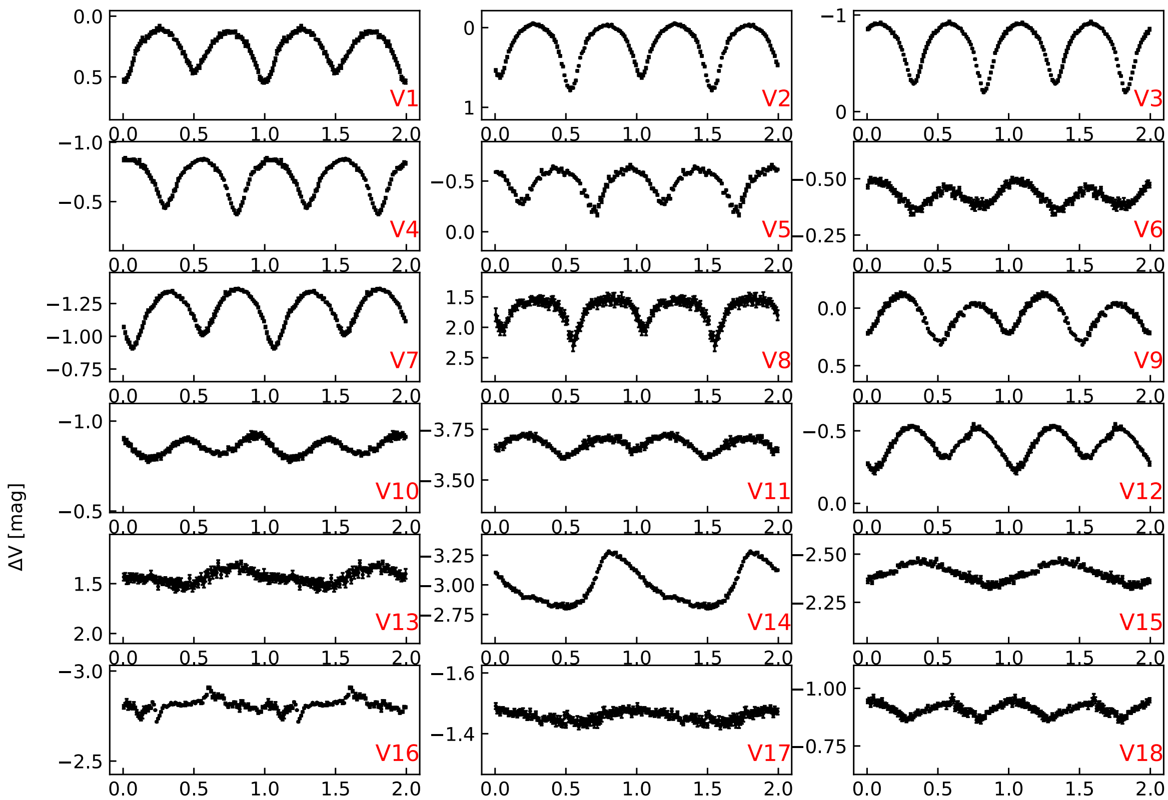

Figure 3. The phased light curves of periodic variable stars.

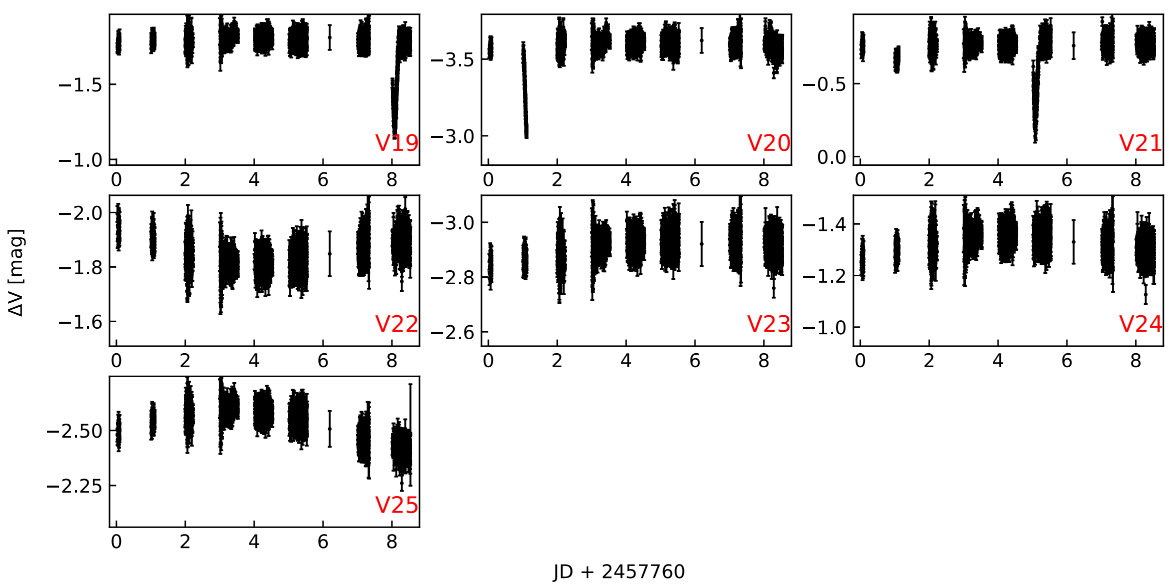

Figure 4. The light curves of long-period variable stars.

period variable stars, and the light curves of these variables are displayed in Figure 4.

For the amplitudes of the periodic variables, phased data were sorted from small to large first, then we averaged the sorted data with a sampling interval of 60 data points using the moving average method (Shan et al. 2022). Next, the amplitude of the variation in periodic variables was calculated by subtracting the minimum values from the maximum values.

We did almost the same operation for the amplitudes of other detected variables, except that the data were sorted by Julian Dates. Bai et al. (2019) report the stellar effective temperature regression for the second Gaia data release by applying a supervised machine-learning algorithm, based on the combination of the stars in four spectroscopic surveys: the Large Sky Area Multi-Object Fiber Spectroscopic Telescope (LAMOST), Sloan Extension for Galactic Understanding and Exploration (SEGUE), Apache Point Observatory Galactic Evolution Experiment (APOGEE) and Radial Velocity Extension. We have given the effective temperatures of most variables by cross-matching the coordinates with those from Bai et al. (2019), except for V11 and V15, which have no values of effective temperatures listed in this table due to inconformity with source selection criteria of Bai et al. (2019). The effective temperature of these variable stars ranges from 4200 to 6700 K, corresponding to the spectral types of K - F.

The identified variables were cross-checked with the International Variable Star Index (VSX[6]) and the catalog of Gaia DR3 Part 4 Variability (Gaia Collaboration 2022), and most variables were found to match with the online catalogs except one star, V18, which implies that in our sample only V18 is a new discovery. The periods, amplitudes and shapes of the light curves of known stars produced by this work are mostly consistent with those given on the VSX website. We found an about 0.5 mag eclipse appeared in the light curve of V21, which implies that it could be an Algol-type eclipsing binary rather than a BY Draconis-type variable star as reported by Mochejska et al. (2008).

3.1. Cluster Membership of the Detected Variables

To identify the cluster membership of the detected variable stars in this work, we cross-matched our coordinates of variable stars with Cantat-Gaudin et al. (2020, CG20), which provided 857 cluster members with probabilities over 70% of OC NGC 188 using the membership assignment code Unsupervised Photometric Membership Assignment in Stellar Clusters (UPMASK, Krone-Martins & Moitinho 2014) based on the Gaia Data Release 2 (DR2) database (Evans et al. 2018). Fourteen variables are identified as cluster members with 100% membership probabilities and the others are possible field stars for their larger proper motion (pm) in the decl. direction compared with cluster members.

Tarricq et al. (2022) point out that Cantat-Gaudin et al. (2018) might ignore the cluster members in the peripheral regions of OCs. In order not to miss the cluster member variables, we took advantage of Gaia DR3 (Gaia Collaboration 2022), which provides more exquisite astrometric precision than Gaia DR2, to revisit the memberships of the detected variable stars. First, we queried a cone of 30′ radius around the cluster center with non-zero astrometric and photometric parameters, as well as errors in G mag smaller than 0.005, to create Basic Sources. Figure 5(a) presents the spatial positions of the Basic Sources and the 25 variable stars. The Basic Sources and variables are represented in gray and red/blue dots respectively. The cluster members are obviously concentrated in the spatial center. In proper motion space, as featured in Figure 5(b), we set a blue circular region centered on (pm RA, pm DE) = (−2.307, −0.960) mas yr^{-1} with radius 1.0 mas yr^{-1} as the selection criteria, and fifteen variable stars are contained in the circle which is marked in red dots, including all the fourteen variables identified in the preceding paragraph and V9. Then we checked all the stellar parameters of the fifteen stars in the other subgraphs in Figure 5. In Figure 5(a), most red dots are concentrated in the center of the subgraph, while V22 and V9 are two slightly distant dots. Figure 5(c) is the histogram of parallax (ω) and Figure 5(d) presents the observed color–magnitude diagram (CMD) without reddening considered. None of the fifteen stars can be excluded as non-members. To confirm the membership of V9, we checked the catalog of Cantat-Gaudin et al. (2018), which provided the membership probabilities for 883 sources in the field of NGC 188 using UPMASK, but no records were found. However, we found that Platais et al. (2003) classified V9 as a possible member star (the probability is 73%) using astrometry from the Tycho-2 catalog.

The absolute magnitude M_G versus intrinsic color item $G_{\rm BP} - G_{\rm RP}$ CMD for the OC NGC 188 is shown in Figure 6. The absolute magnitude M_G is transformed by the observational magnitude G mag and the distance of each member star. The distances are referenced from Bailer-Jones et al. (2021) estimated by probabilistic methods using a 3D a priori model of the Galaxy based on Gaia Early Data Release 3 (EDR3). We calculated the extinction coefficients A_G, $A_{\rm BP}$ and $A_{\rm RP}$ as follows

$$\begin{aligned} A_M/A_V &= c_{1M} + c_{2M}(G_{\rm BP} - G_{\rm RP}) + c_{3M}(G_{\rm BP} - G_{\rm RP})^2 \\ &+ c_{4M}(G_{\rm BP} - G_{\rm RP})^3 \\ &+ c_{5M}A_V + c_{6M}{A_V}^2 + c_{7M}(G_{\rm BP} - G_{\rm RP})A_V. \end{aligned} \tag{1}$$

This is the transformation relation for Gaia bands defined by Gaia Collaboration et al. (2018), where M represents G, BP or RP band, and $c_{1...7M}$ means a set of coefficients.

The Padova theoretical isochrone (Bressan et al. 2012) is represented by a black solid line in Figure 6. For the metallicity, we adopted the metal value [Fe/H] = + 0.064 ± 0.018 dex provided by WIYN/Hydra spectra of Sun et al. (2022). Other cluster parameters adopted are taken from Cantat-Gaudin et al. (2020) ($\log(t) = 9.85$ yr, $Z = 0.0152$, $V - M_V = 11.15$ mag, $A_V = 0.21$ mag).

[6] http://www.aavso.org/vsx/

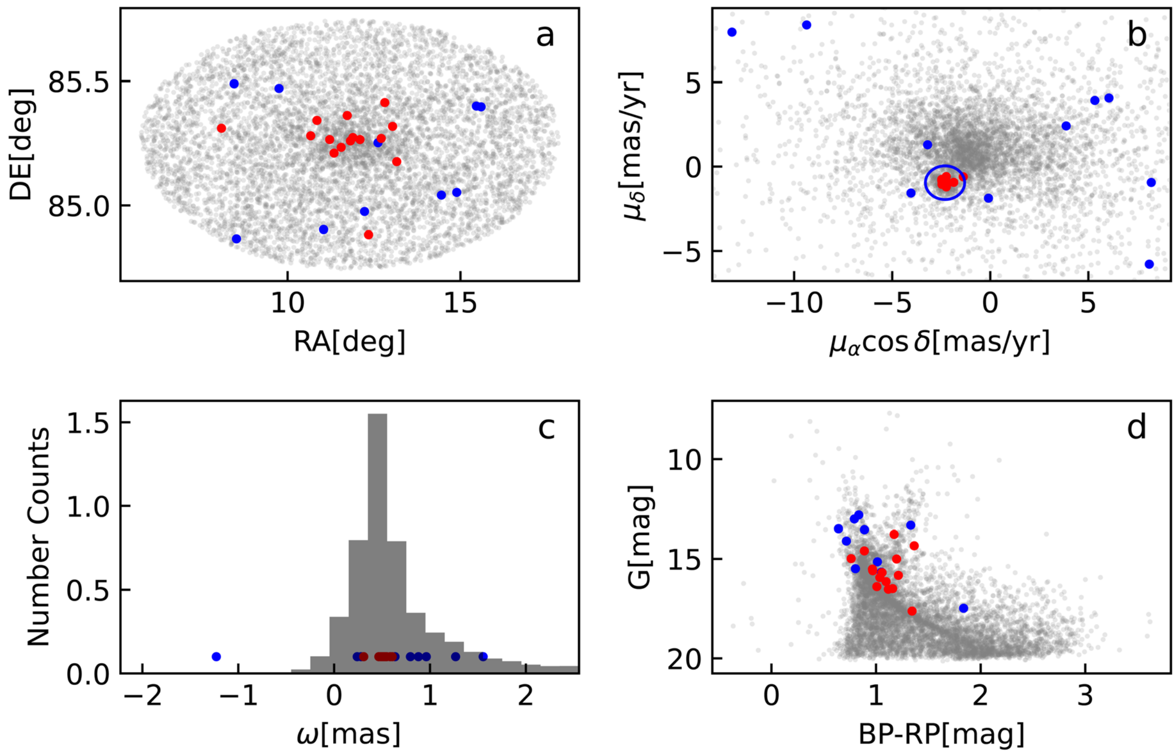

Figure 5. (a) Spatial distribution for the stars in the field of NGC 188 and 25 variable stars; (b) proper motion distribution; (c) histogram of parallax (ω); (d) observed CMD without reddening considered. In the panels, light gray dots represent the Basic Sources of Gaia DR3. Red and blue dots correspond to the variable members and non-members, respectively.

4. Results and Discussion

4.1. Compared to Previous Works

The four well-known W UMa variable stars identified by Hoffmeister (1964), V1–V4, are easily detected in our observations. The suspected variable NSV 395 was not included in our FOV. All the variables identified by Kaluzny & Shara (1987) were detected in our observations, but only the light curves of three variables (V5, V6, and V12) showed large enough variabilities. NSV 15158 (V25) was confirmed in this work. The variations of the variables discovered by Xin et al. (2002) were also detected in this work, except for two outside of the FOV. None of the faint variables found by Kafka & Honeycutt (2003) were confirmed in our catalog. Among the eight variables identified by Zhang et al. (2004), three of them were outside of the FOV, and no variations were found in the other three light curves; only two variables (V9, V15) were confirmed in this work. It is difficult to observe the variations of the BY Draconis type variables discovered by Mochejska et al. (2008) due to the telescope's limitation. The eclipsing binary (V13) and one BY Draconis type star (V21) from Mochejska et al. (2008) were detected in this work. Among the eighteen variables of Popov et al. (2013), eleven were out of the FOV, and the light curves of two variables were flat in our observations; the other five were confirmed in this work. The four suspected variables are detected in our observation, while NSV 15164 is saturated, and the light curves of the other three variables did not show changes. None of the variables discovered by the TAROT Suspected Variable Star Catalog, ver. 1 (TSVSC1) are confirmed by this work. For the two variables detected by ASAS-SN, the detached eclipsing binary (V20) was detected, but there were no variations detected in the light curve of another variable in this work. All the detected 24 known variables are listed in Table 2. Among the 24 detected known variables in the field of NGC 188, well-phased light curves were recorded for the first 17 variables listed in Table 2 as shown in Figure 3. As displayed in Figure 4, the observational durations of the other seven variables are not long enough to determine the period of these variable stars. All the memberships of the detected variables are listed in Table 2. We did not investigate the known variable stars if our data were basically consistent with the previous conclusions.

V16 and V17 were found as variable stars by Popov et al. (2013). Because of the low amplitudes of their light variations, the classifications for the two stars still remain unknown. V16 is a certain foreground field star and is a spectroscopic variable star classified by Tian et al. (2020) based on LAMOST Data Release 4 (DR4). V17 is a certain blue straggler star (BSS)

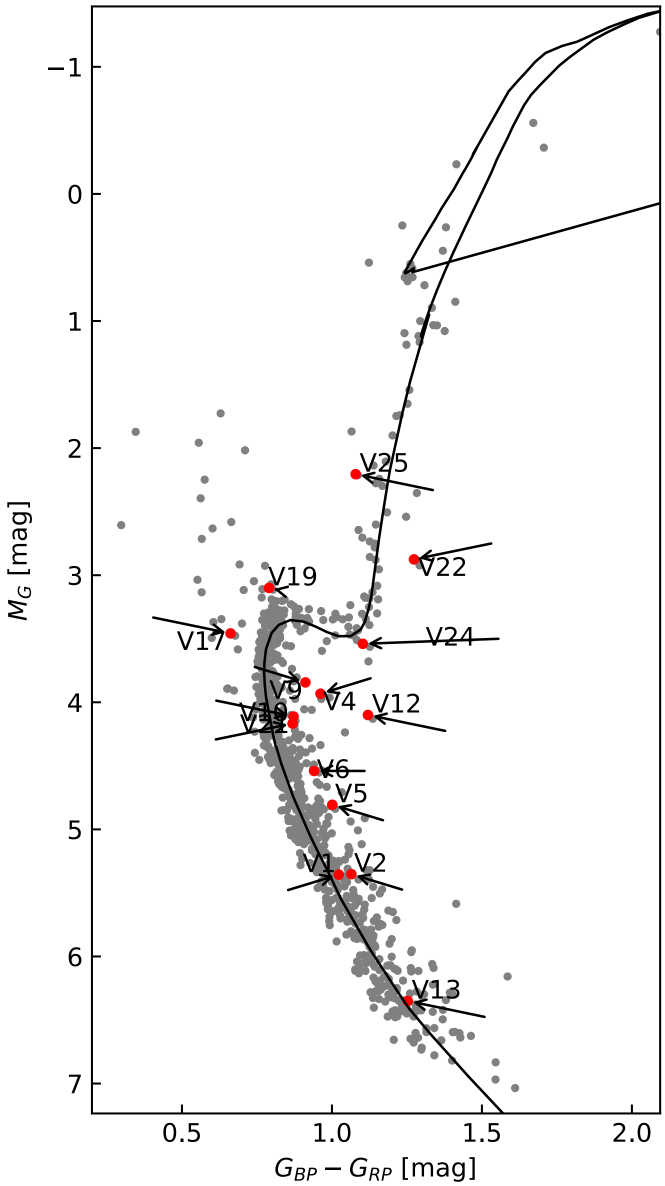

Figure 6. CMD for cluster members of NGC 188 with the positions of the 16 cluster variables marked in red color. The cluster members are provided by CG20 with probabilities over 70%. The cluster parameters used in the Padova theoretical isochrone fitting come from CG20 and Sun et al. (2022).

based on the location of the CMD, and it was classified as a single-lined BSS with rapid rotation by Geller et al. (2009).

V21 was classified as a BY Draconis type variable by Mochejska et al. (2008). It was detected by our observations because an about 0.5 mag eclipse appeared in the light curve of this star, which implies that it might be an Algol-type eclipsing binary. The location of this star in our absolute M_G versus $G_{\rm BP} - G_{\rm RP}$ CMD also reinforces this view. More observations for this star are needed to determine its period and properties.

4.2. Classification of New Variable

One new periodic variable star (V18) is identified in this work. The phased light curves are depicted in Figure 3, and the basic parameters for the variable are listed in Table 2. As discussed above, this is a field star with definite variations of brightness. Based on the distances of the star, V18 is a field star mixed with cluster members. We considered the period, amplitude, light-curve shape, effective temperature and positions on the CMD to classify the variable stars obtained in this study. We checked the star's position on the CMD and compared with the statistical positions of the periodic variable stars on the CMDs given by Gaia Collaboration et al. (2019), and found it could be a W UMa binary.

5. Conclusions

In this paper, we have presented the time-series *V*-band photometric survey of the OC NGC 188, with particular emphasis on variable stars. The results of this study are the following:

1. We detected 25 variable stars in a 55 $\times$ 45 arcmin^2 FOV around the cluster, including one new variable. Their memberships are determined by the research of CG20 and reconfirmed by Gaia DR3. Most results are consistent with CG20, except V9, which is a possible cluster member in our research. Our results suggest that 15 variables are cluster members while the other 14 stars belong to the field star population.
2. Based on the behaviors and periods of the light curves as well as their positions on the CMD, we discussed the classifications of the 25 variable stars. Most results of the known variables are coincident with the VSX catalog, except V21 (V0769 Cep), which is preferred to be an EA-type eclipsing binary rather than a BY Draconis type variable star. The new variable is likely to be a W UMa eclipsing star. The detection and analysis of the variable stars in the old OC NGC 188 yield valuable samples, especially for the study of W UMa stars.

Acknowledgments

We are grateful to an anonymous referee for valuable comments which improved the paper significantly. This work has been financially supported by the Resource sharing platform construction project of Xinjiang Uygur Autonomous Region (No. PT2306) and the Chinese Academy of Sciences (CAS) "Light of West China" Program (No. 2020-XBQNXZ-016, 2022-XBQNXZ-016). This work has made use of data from the European Space Agency (ESA) mission Gaia (https://www.cosmos.esa.int/gaia), processed by the Gaia Data Processing and Analysis Consortium (DPAC, https://www.cosmos.esa.int/web/gaia/dpac/consortium). The CCD photometric data of NGC 188 were obtained with the Nanshan One-meter Wide-field Telescope administered by Xinjiang Astronomical Observatory.

ORCID iDs

Fang-Fang Song https://orcid.org/0000-0002-5926-4137

References

Bai, C.-H., Feng, G.-J., Zhang, X., et al. 2020, RAA, 20, 211
Bai, Y., Liu, J., Bai, Z., Wang, S., & Fan, D. 2019, AJ, 158, 93
Bailer-Jones, C. A. L., Rybizki, J., Fouesneau, M., Demleitner, M., & Andrae, R. 2021, AJ, 161, 147
Bertin, E., & Arnouts, S. 1996, A&AS, 117, 393
Bonatto, C. 2019, MNRAS, 483, 2758
Bonatto, C., Bica, E., & Santos, J. F. C. 2005, A&A, 433, 917
Bressan, A., Marigo, P., Girardi, L., et al. 2012, MNRAS, 427, 127
Cantat-Gaudin, T., Anders, F., Castro-Ginard, A., et al. 2020, A&A, 640, A1
Cantat-Gaudin, T., Jordi, C., Vallenari, A., et al. 2018, A&A, 618, A93
Cohen, R. E., Geller, A. M., & von Hippel, T. 2020, AJ, 159, 11
Czesla, S., Schröter, S., Schneider, C. P., et al. 2019, PyA: Python astronomy-related packages, Astrophysics Source Code Library, ascl:1906.010
Evans, D. W., Riello, M., De Angeli, F., et al. 2018, A&A, 616, A4
Fornal, B., Tucker, D. L., Smith, J. A., et al. 2007, AJ, 133, 1409
Friel, E. D., Jacobson, H. R., & Pilachowski, C. A. 2010, AJ, 139, 1942
Gaia Collaboration 2022, VizieR On-line Data Catalog: yCat, I/355
Gaia Collaboration, Babusiaux, C., van Leeuwen, F., et al. 2018, A&A, 616, A10
Gaia Collaboration, Eyer, L., Rimoldini, L., et al. 2019, A&A, 623, A110
Gaia Collaboration, Prusti, T., de Bruijne, J. H. J., et al. 2016, A&A, 595, A1
Geller, A. M., Mathieu, R. D., Harris, H. C., & McClure, R. D. 2008, AJ, 135, 2264
Geller, A. M., Mathieu, R. D., Harris, H. C., & McClure, R. D. 2009, AJ, 137, 3743
Gillen, E., Hillenbrand, L. A., Stauffer, J., et al. 2020, MNRAS, 495, 1531
Hills, S., von Hippel, T., Courteau, S., & Geller, A. M. 2015, AJ, 149, 94
Hoffmeister, C. 1964, AN, 288, 49
Kafka, S., & Honeycutt, R. K. 2003, AJ, 126, 276
Kaluzny, J. 1990, AcA, 40, 61
Kaluzny, J., & Shara, M. M. 1987, ApJ, 314, 585
Krone-Martins, A., & Moitinho, A. 2014, A&A, 561, A57
Li, C.-Y., Esamdin, A., Zhang, Y., et al. 2021, RAA, 21, 068
Ma, S.-G., Esamdin, A., Ma, L., et al. 2018, Ap&SS, 363, 68
Mochejska, B. J., Stanek, K. Z., Sasselov, D. D., et al. 2008, AcA, 58, 263
Monteiro, H., Dias, W. S., Moitinho, A., et al. 2020, MNRAS, 499, 1874
Özeren, F. F., Arslan, Ö., Küçük, İ., & Oralhan, İ. A. 2014, NewA, 32, 36
Piskunov, A. E., Kharchenko, N. V., Röser, S., Schilbach, E., & Scholz, R.-D. 2006, A&A, 445, 545
Platais, I., Kozhurina-Platais, V., Mathieu, R. D., Girard, T. M., & van Altena, W. F. 2003, AJ, 126, 2922
Popov, A. A., Krushinsky, V. V., Avvakumova, E. A., et al. 2013, OEJV, 157, 1
Sarajedini, A., von Hippel, T., Kozhurina-Platais, V., & Demarque, P. 1999, AJ, 118, 2894
Shan, Z., Yang, J., Sanjuán, M. A. F., Wu, C., & Liu, H. 2022, EPJP, 137, 50
Song, F.-F., Esamdin, A., Ma, L., et al. 2016, RAA, 16, 154
Sun, Q., Deliyannis, C. P., Twarog, B. A., et al. 2022, MNRAS, 513, 5387
Tarricq, Y., Soubiran, C., Casamiquela, L., et al. 2022, A&A, 659, A59
Tian, Z., Liu, X., Yuan, H., et al. 2020, ApJS, 249, 22
Wang, J., Ma, J., Wu, Z., Wang, S., & Zhou, X. 2015, AJ, 150, 61
Xin, Y., Zhang, X.-B., & Deng, L.-C. 2002, ChJAA, 2, 481
Zacharias, N., Finch, C. T., Girard, T. M., et al. 2013, AJ, 145, 44
Zechmeister, M., & Kürster, M. 2009, A&A, 496, 577
Zhang, X. B., Deng, L., Zhou, X., & Xin, Y. 2004, MNRAS, 355, 1369